一般社団法人　電子情報通信学会
THE INSTITUTE OF ELECTRONICS,
INFORMATION AND COMMUNICATION ENGINEERS

信学技報
IEICE Technical Report
RCS2016-290 (2017-03)

Blind Selected Mapping Technique for Space-Time Block Coded Transmit Diversity with Transmit Frequency-Domain Equalization

Amnart Boonkajay † and Fumiyuki Adachi ‡

† ‡ Research Organization of Electrical Communication (ROEC), Tohoku University
2-1-1 Katahira, Aoba-ku, Sendai, Miyagi, 980-8577 Japan
E-mail: † amnart@riec.tohoku.ac.jp ‡ adachi@ecei.tohoku.ac.jp

Abstract Peak-to-average power ratio (PAPR) reduction is still an important issue in the next-generation mobile communication networks using higher frequency bands. Recently, we have proposed a PAPR reduction technique called blind selected mapping (blind SLM), which does not require side-information transmission and is able to reduce the PAPR effectively without bit-error rate (BER) degradation, for single-antenna transmission and for space-time block coded transmit diversity (STBC-TD). We exploited the fact that PAPR of the signal after STBC encoding and that of before STBC encoding are the same. However, if STBC-TD is combined with transmit frequency-domain equalization (Tx-FDE), the PAPR of transmit signal from each antenna becomes different from those signals before STBC encoding. This is because the transmit blocks are added/subtracted and multiplied with the FDE weights. In this paper, a blind SLM technique is applied to STBC-TD with Tx-FDE. Both orthogonal frequency division multiplexing (OFDM) transmission and single-carrier (SC) transmission (equivalent to discrete Fourier transform (DFT)-precoded OFDM transmission) are considered. Performance of the blind SLM for STBC-TD with Tx-FDE is evaluated by computer simulation, where the simulation results show that blind SLM techniques can lower the PAPR of STBC-TD with Tx-FDE without causing BER degradation.

Keyword Space-time block coded transmit diversity (STBC-TD), peak-to-average power ratio (PAPR), selected mapping (SLM), frequency-domain equalization (FDE)

1. Introduction

Higher frequency bands e.g. centimeter and millimeter waves, where abundant bandwidth remains unused, will be used in the next-generation mobile communication networks [1]. Therefore, peak-to-average power ratio (PAPR) reduction is still an important issue since the high power amplifier (HPA) suffers from low amplification efficiency when operating at high carrier frequency [2]. PAPR properties of orthogonal frequency division multiplexing (OFDM) and single-carrier (SC) have been well studied [3]. OFDM waveform generally has higher PAPR than SC waveform. However, PAPR of SC waveform increases due to high-level data modulation and when the SC signal is generated by mean of discrete Fourier transform (DFT)-precoded OFDM [4].

Among various PAPR reduction techniques, selected mapping (SLM) [5] is well-known as an efficient, simple PAPR reduction technique. SLM generates the transmit waveform candidates by multiplying the original signal with the various phase rotation patterns, then select the waveform with the lowest PAPR. The proposed SLM in [5] is originally for OFDM. We recently proposed the blind SLM for filtered SC [6-7], where the phase rotation is conducted in time domain. Maximum likelihood (ML) phase estimation or 2-step estimation based on Viterbi algorithm [8] can be employed at the receiver and hence no side-information transmission is required.

Space-time block-coded transmit diversity (STBC-TD) [9] is a well-known powerful technique to improve the signal transmission quality in a fading environment. Blind SLM for STBC-TD [10] was studied by exploiting a fact that the PAPR of signals before STBC encoding and after STBC encoding are the same. STBC-TD is typically equipped with receive frequency-domain equalization (Rx-FDE) and is able to support arbitrary number of receive antennas, but transmission rate is reduced if the number of transmit antennas increases. On the other hand, STBC-TD equipped with transmit FDE (Tx-FDE) [11] can support an arbitrary number of transmit antennas. However, the PAPR of signals before encoding and after encoding become different because of addition/subtraction operation and multiplication of FDE weights (note that only complex conjugate operation is involved in the case of STBC-TD without Tx-FDE).

In this paper, we study an application of blind SLM to STBC-TD with Tx-FDE. Both OFDM and SC transmissions are considered. In the SLM stage, phase rotation is applied prior to STBC encoding and Tx-FDE in order to preserve the STBC code orthogonality. Phase rotation pattern is selected in order to minimize the maximum instantaneous PAPR among all transmit antennas (hereinafter called minimax criterion). Performance of the blind SLM for STBC-TD with Tx-FDE is evaluated by computer simulation in order to confirm that the PAPR can be reduced with no significant BER degradation.

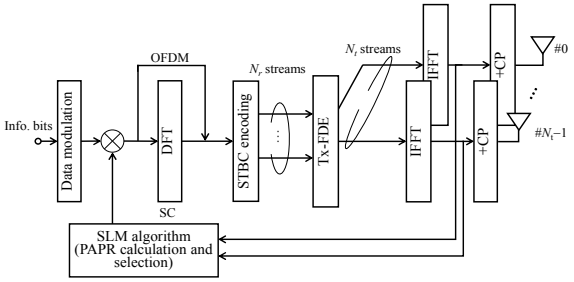

Fig. 1 Transmitter.

Table 1 STBC encoding parameters.

N_t	N_r	J	Q	R_{STBC}
arbitrary	1	1	1	1
	2	2	2	1
	3	3	4	3/4
	4	3	4	3/4

2. STBC-TD transmitter with Tx-FDE and blind SLM

STBC-TD transmitter with Tx-FDE and blind SLM is illustrated by Fig. 1. Point-to-point transmission is assumed in this paper for simplicity. The transmitter is equipped with N_t transmit antennas, and the receiver is equipped with N_r receive antennas.

2.1. Transmit signal representation

We begin with J blocks of N_c-length data-modulated transmit symbols $\{d_j(n); n=0\sim N_c-1, j=0\sim J-1\}$. Phase rotation is employed to the data-modulated blocks. A common phase rotation pattern $\{ p_{\hat{m}}(n) ; n=0\sim N_c-1\}$ is selected by SLM algorithm where $\hat{m} \in 0\sim M-1$ and M is the number of available phase rotation patterns. We assume $\hat{m}$ to be the same for all J blocks. The selection criterion of $\{p_{\hat{m}}(n)\}$ will be described in details in Section 2.2. J blocks of N_c-length phase-rotated symbols $\{ d_{j,\hat{m}}(n) ; n=0\sim N_c-1, j=0\sim J-1\}$ is

$$d_{j,\hat{m}}(n) = p_{\hat{m}}(n) d_j(n). \tag{1}$$

In case of SC transmission, $\{d_{j,\hat{m}}(n)\}$ is then transformed into frequency domain by N_c-point DFT, yielding J blocks of frequency components $\{ D_{j,\hat{m}}(k) ; k=0\sim N_c-1, j=0\sim J-1\}$. The frequency component blocks before STBC encoding $\{D_{j,\hat{m}}(k)\}$ is expressed by

$$D_{j,\hat{m}}(k) = \begin{cases} \dfrac{1}{\sqrt{N_c}} \displaystyle\sum_{n=0}^{N_c-1} d_{j,\hat{m}}(n) \exp(-i2\pi \frac{kn}{N_c}) & \text{for SC} \\ d_{j,\hat{m}}(k) & \text{for OFDM} \end{cases}, \tag{2}$$

where $i = \sqrt{-1}$. Next, J blocks of frequency component $\{D_{j,\hat{m}}(k)\}$ are encoded by STBC encoding, yielding N_r parallel streams of Q encoded frequency component blocks. The STBC encoding process for each frequency index k can be represented by an $N_r \times Q$ matrix $\mathbf{X}_{\hat{m}}(k)$ [9]. $\mathbf{X}_{\hat{m}}(k)$ depends on N_r and is expressed by [9,11].

$$\mathbf{X}_{\hat{m}}(k) = \begin{cases} D_{0,\hat{m}}(k) & \text{if } N_r = 1 \\ \begin{bmatrix} D_{0,\hat{m}}(k) & -D^*_{1,\hat{m}}(k) \\ D_{1,\hat{m}}(k) & D^*_{0,\hat{m}}(k) \end{bmatrix} & \text{if } N_r = 2 \\ \begin{bmatrix} D_{0,\hat{m}}(k) & -D^*_{1,\hat{m}}(k) & -D^*_{2,\hat{m}}(k) & 0 \\ D_{1,\hat{m}}(k) & D^*_{0,\hat{m}}(k) & 0 & -D^*_{2,\hat{m}}(k) \\ D_{2,\hat{m}}(k) & 0 & D^*_{0,\hat{m}}(k) & D^*_{1,\hat{m}}(k) \end{bmatrix} & \text{if } N_r = 3 \\ \begin{bmatrix} D_{0,\hat{m}}(k) & -D^*_{1,\hat{m}}(k) & -D^*_{2,\hat{m}}(k) & 0 \\ D_{1,\hat{m}}(k) & D^*_{0,\hat{m}}(k) & 0 & -D^*_{2,\hat{m}}(k) \\ D_{2,\hat{m}}(k) & 0 & D^*_{0,\hat{m}}(k) & D^*_{1,\hat{m}}(k) \\ 0 & D_{2,\hat{m}}(k) & -D_{1,\hat{m}}(k) & D_{0,\hat{m}}(k) \end{bmatrix} & \text{if } N_r = 4 \end{cases} \tag{3}$$

In addition, the STBC encoding parameters N_r, J and Q, and the corresponding coding rate $R_{\mathrm{STBC}}=J/Q$, are shown in Table 1.

Tx-FDE is applied after STBC encoding, where the Tx-FDE weight matrix at frequency index k can be represented by an $N_t \times N_r$ matrix $\mathbf{W}_t(k)$. In this paper, we use the minimum mean-square error based FDE (MMSE-FDE) for both OFDM and SC transmissions. The FDE weight at the n_t-th row and the n_r-th column, $W_t(k;n_t,n_r)$, is expressed by [11]

$$W_t(k;n_t,n_r) = \frac{H^*(k;n_r,n_t)}{\dfrac{1}{N_r}\displaystyle\sum_{n_r=0}^{N_r-1} \left|H(k;n_r,n_t)\right|^2 + \left(\dfrac{E_s}{N_0}\right)^{-1}}, \tag{4}$$

where $H(k;n_r,n_t)$ is an element at the n_t-th row and the n_r-th column of multi-input multi-output (MIMO) channel transfer function at the $\mathbf{H}(k)$, $k=0\sim N_c-1$. E_s represents symbol energy and N_0 is one-sided noise power spectrum density, respectively. The frequency-domain transmit signal matrix at frequency index k, $\mathbf{S}_{\hat{m}}(k)$, with the dimension of $N_t \times Q$ is given by

$$\mathbf{S}_{\hat{m}}(k) = A\mathbf{W}_t(k)\mathbf{X}_{\hat{m}}(k), \tag{5}$$

where A represents power normalization factor and is expressed by

$$A = \frac{1}{\sqrt{\dfrac{1}{N_c}\displaystyle\sum_{k=0}^{N_c-1}\sum_{n_t=0}^{N_t-1}\sum_{n_r=0}^{N_r-1}\left|W_t(k;n_t,n_r)\right|^2}}, \tag{6}$$

After applying Tx-FDE, the q-th frequency-domain block at the n_t-th transmit antenna $\{ S_{\hat{m}}(k;n_t,q) ; k=0\sim N_c-1\}$ is transformed back to time-domain transmit signal $\{ s_{\hat{m}}(n;n_t,q) ; n=0\sim N_c-1\}$ by N_c-point inverse fast Fourier transform (IFFT), yielding

$$s_{\hat{m}}(n;n_t,q) = \frac{1}{\sqrt{N_c}} \sum_{n=0}^{N_c-1} S_{\hat{m}}(k;n_t,q) \exp(i2\pi \frac{kn}{N_c}). \tag{7}$$

Finally, the last N_g samples of transmit block are copied as

a cyclic prefix (CP) and inserted into the guard interval (GI), then a CP-inserted signal block of N_g+N_c samples is transmitted from each transmit antenna.

2.2. Blind SLM algorithm

Assuming that an N_c-length time-domain transmit block is represented by $\{s(n);\ n=0\sim N_c-1\}$, PAPR is calculated over a V-times oversampled block, which is

$$\mathrm{PAPR}(\{s(n)\}) = \frac{\max\{|s(n)|^2, n=0,\frac{1}{V},\frac{2}{V},...,N_c-1\}}{\frac{1}{N_c}\sum_{n=0}^{N_c-1}|s(n)|^2}. \qquad (8)$$

Transmit waveform of STBC-TD with Tx-FDE is different from that of STBC-TD with Rx-FDE since $S_{\hat{m}}(k;n_t,q)$ is generated based on addition of $D_{j,\hat{m}}(k)$ multiplied with $W_t(k;n_t,n_r)$, resulting in the frequency-domain output block at each transmit antenna is neither $\pm D_{j,\hat{m}}(k)$ nor $\pm D^*_{j,\hat{m}}(k)$. In order to keep blind data detection simple, the multiplication of phase rotation in STBC-TD with Tx-FDE should follows the following restrictions.

- Phase rotation should be conducted prior to STBC encoding and Tx-FDE. This can avoid the large number of candidates generation in phase rotation pattern estimation at the receiver since it does not need to consider all combination of transmit/receive signals and phase rotation patterns at each receive antenna.
- Same phase rotation pattern should be applied to $\{d_j(n)\}$ in order to preserve the STBC code orthogonality. In addition, the phase rotation patterns can be different for different j blocks.

A set of M different unit-magnitude polyphase rotation patterns $\{p_m(n);\ n=0\sim N_c-1,\ m=0\sim M-1\}$ is generated in random approach as $p_m(n)\in\{e^{i0}, e^{i(2\pi/3)}, e^{i(4\pi/3)}\}$, except the first pattern is defined as $\{p_0(n)=e^{i0};\ n=0\sim N_c-1\}$ [7-8,10]. The selected phase rotation pattern $\{p_{\hat{m}}(n);\ n=0\sim N_c-1\}$ with the corresponding pattern index $\hat{m}$ is selected so as to minimize the maximum PAPR of transmit waveform among N_t transmit antennas and Q blocks (i.e., minimax criterion), that is

$$\hat{m} = \arg\min_{m=0,1,...,M-1}\left(\max_{\substack{n_t=0,1,...,N_t-1\\ q=0,1,...,Q-1}} \mathrm{PAPR}\left(\{s_m(n;n_t,q)\}\right)\right), \qquad (9)$$

where $\{s_m(k;n_t,q);k=0\sim N_c-1\}$ is the the q-th time-domain transmit block at the n_t-th transmit antenna corresponding to the m-th phase rotation pattern. It is seen from (9) that the common phase rotation pattern is used for all $N_t\times Q$ transmit waveforms, indicating that the degree of freedom in waveform candidates generation decreases when N_t and/or N_r increase. In addition, we can alternatively select a phase rotation pattern from available B patterns for each J block, but we have confirmed by computer simulation that it achieves the same PAPR performance as selecting a common pattern for all J blocks from $M=B^J$ patterns.

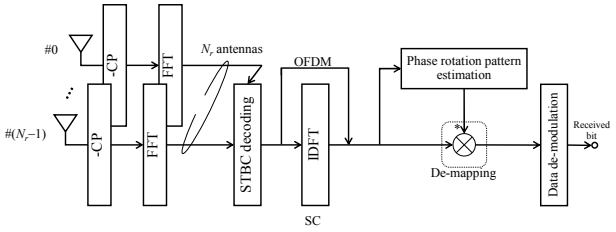

Fig. 2 Receiver.

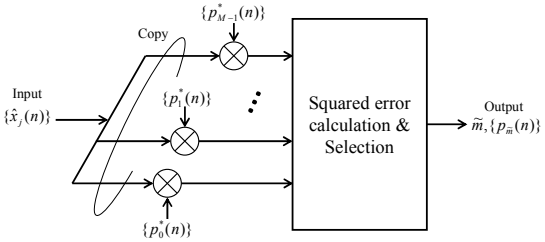

Fig. 3 Phase rotation pattern estimation algorithm.

3. Receiver with phase rotation estimation

The receiver of STBC-TD with Tx-FDE and blind SLM, equipped with N_r receive antennas, is illustrated by Fig. 2. It can be seen that the receiver consists of two main processes; STBC decoding and phase rotation pattern estimation.

The wireless channel is assumed to be a symbol-spaced L-path frequency-selective block Rayleigh fading channel, where its impulse response between the n_t-th transmit antenna and the n_r-th receive antenna is given by

$$h_{n_r,n_t}(\tau) = \sum_{l=0}^{L-1} h_{n_r,n_t,l}\,\delta(\tau-\tau_{n_r,n_t,l}), \qquad (10)$$

where $h_{n_r,n_t,l}$ and $\tau_{n_r,n_t,l}$ are complex-valued path gain and time delay of the l-th path, respectively. In addition, $h_{n_r,n_t,l}$ is assumed to be the same for Q encoded block in this paper for simplicity. The q-th block received signal at the n_r-th antenna $\{r(n;n_r,q);n=0\sim N_c-1\}$ is expressed by

$$r(n;n_r,q) = \sqrt{\frac{2E_s}{T_s}}\sum_{n_t=0}^{N_t-1}\sum_{l=0}^{L-1} h_{n_r,n_t,l}\,s(n-\tau_{n_r,n_t,l};n_t,q) + z(n;n_r,q), \qquad (11)$$

where $z(n;n_r,q)$ is an additive white Gaussian noise (AWGN) having zero mean and the variance of $2N_0/T_s$ with T_s is symbol duration. After CP removal, $\{r(n;n_r,q)\}$ is transformed into frequency domain by N_c-point FFT. The frequency-domain received signal at frequency index k can be written as an $N_r\times Q$ matrix $\mathbf{R}(k)$, which is given by

$$\mathbf{R}(k) = \sqrt{\frac{2E_s}{T_s}}\mathbf{H}(k)\mathbf{S}_{\hat{m}}(k) + \mathbf{Z}(k), \qquad (12)$$

where $\mathbf{Z}(k)$ is the frequency-domain noise matrix obtained by applying N_c-point FFT to $z(n;n_r,q)$.

Next, STBC decoding is carried out to obtain spatial diversity gain. The frequency-domain decoded block $\{\hat{X}_j(k);k=0\sim N_c-1,j=0\sim J-1\}$ is determined by the following STBC decoders [11], which employ only

addition/subtraction and complex-conjugate operations:

$$\hat{X}_0(k) = R(k;0,0) \qquad \text{if } N_r = 1, \tag{13a}$$

$$\begin{bmatrix} \hat{X}_0(k) \\ \hat{X}_1(k) \end{bmatrix} = \begin{bmatrix} R(k;0,0) + R^*(k;1,1) \\ R(k;0,1) - R^*(k;1,0) \end{bmatrix} \qquad \text{if } N_r = 2, \tag{13b}$$

$$\begin{bmatrix} \hat{X}_0(k) \\ \hat{X}_1(k) \\ \hat{X}_2(k) \end{bmatrix} = \begin{bmatrix} R(k;0,0) + R^*(k;1,1) + R^*(k;2,2) \\ R(k;0,1) - R^*(k;1,0) + R^*(k;3,2) \\ R(k;0,2) - R^*(k;2,0) - R^*(k;3,1) \end{bmatrix} \qquad \text{if } N_r = 3, \tag{13c}$$

$$\begin{bmatrix} \hat{X}_0(k) \\ \hat{X}_1(k) \\ \hat{X}_2(k) \end{bmatrix} = \begin{bmatrix} R(k;0,0) + R^*(k;1,1) + R^*(k;2,2) + R(k;0,0) \\ R(k;0,1) - R^*(k;1,0) - R(k;2,3) + R^*(k;3,2) \\ R(k;0,2) + R(k;1,3) - R^*(k;2,0) - R^*(k;3,1) \end{bmatrix} \text{ if } N_r = 4. \tag{13d}$$

After STBC decoding, the received blocks before de-mapping $\{\hat{x}_j(n); n=0\sim N_c-1, j=0\sim J-1\}$ is obtained based on different transmission techniques. In SC transmission, $\{\hat{x}_j(n)\}$ is obtained by applying N_c-point inverse DFT (IDFT) to $\{\hat{X}_j(k)\}$, that is

$$\hat{x}_j(n) = \begin{cases} \dfrac{1}{\sqrt{N_c}} \sum_{k=0}^{N_c-1} \hat{X}_j(k) \exp(i2\pi \dfrac{kn}{N_c}) & \text{for SC} \\ \hat{X}_j(n) & \text{for OFDM} \end{cases}. \tag{14}$$

Note that there still exists the phase rotation regarding to SLM in $\{\hat{x}_j(n)\}$. In general, the received symbol blocks before data de-modulation $\{\hat{d}_j(n); n=0\sim N_c-1, j=0\sim J-1\}$ is obtained by employing de-mapping, i.e. multiplying $\hat{x}_j(n)$ by $p_{\tilde{m}}^*(n)$, but it requires side-information transmission. To conduct signal detection without side-information, the receiver employs phase rotation pattern estimation to estimate which pattern is likely to be used at the transmitter. The phase rotation pattern estimation exploits a fact that correct de-mapping makes the received symbols become close to original constellation, resulting in very low squared error from the original constellation [7]. The estimated phase rotation pattern $p_{\tilde{m}}(n)$ with the corresponding pattern index $\tilde{m}$ is determined based on the following equation.

$$\tilde{m} = \arg \min_{\substack{m=0,1,\ldots,M-1, \\ c \in \Psi_{\text{mod}}}} \left(\varepsilon = \sum_{j=0}^{J-1} \sum_{n=0}^{N_c-1} \left| p_m^*(n) \hat{x}_j(n) - c \right|^2 \right), \tag{15}$$

where Ψ_{mod} is the original data-modulated constellation. The estimation in (15) can be conducted by using ML estimation (i.e. exhaustive search) [7] or 2-step estimation using Viterbi algorithm [8], where the latter approach requires much less computational complexity and no significant BER degradation. The ML phase rotation pattern estimation part is depicted in Fig. 3. Finally, the received symbols for data de-modulation $\{\hat{d}_j(n)\}$ is given by

$$\hat{d}_j(n) = p_{\tilde{m}}^*(n) \hat{x}_j(n). \tag{16}$$

4. Performance Evaluation

Numerical and simulation parameters are summarized in Table 2. Channel coding is not considered for simplicity. A set of phase rotation patterns is generated in random approach from polyphase rotations $\{e^{i0}, e^{i2\pi/3}, e^{i4\pi/3}\}$ which are not optimal but sufficient for allowing blind SLM [7-8,10]. In case of transmission with side-information sharing, the required side-information bits are $J\log_2 M$ [6]. N_r is set to be 2 receive antennas since it keeps the STBC coding rate R_{STBC}=1. Performance evaluation is done and discussed in terms of PAPR and BER.

Table 2 Simulation parameters.

Transmitter	Data modulation	16QAM
	No. of subcarriers	N_c=64
	CP length	N_g=16
	No. of transmit antennas	N_t=1~4
	Tx-FDE type	MMSE
SLM parameter	Phase rotation type	Random polyphase $\{e^{i0}, e^{i2\pi/3}, e^{i4\pi/3}\}$
	No. of patterns	M=1~256
Channel	Fading	Frequency-selective block Rayleigh
	Power delay profile	Symbol-spaced, 16-path uniform
Receiver	No. of receive antennas	N_r=2
	Channel estimation	Ideal
	Phase rotation pattern estimation method	ML estimation

4.1. PAPR

PAPR performance is evaluated by measuring the PAPR value at complementary cumulative distribution function (CCDF) equals 10^{-3}, called $\text{PAPR}_{0.1\%}$. Figs. 4(a) and 4(b) show the $\text{PAPR}_{0.1\%}$ versus the number of phase rotation patterns (M) of OFDM and SC transmission with STBC-TD and Tx-FDE, respectively. $\text{PAPR}_{0.1\%}$ of single-antenna OFDM without Tx-FDE (10.6 dB) and single-antenna SC without Tx-FDE (8.4 dB) are also plotted for comparison. The total transmit bit energy-per-N_0 (E_b/N_0) is set to be 10 dB.

The PAPR performance of OFDM transmission is firstly discussed in this section. It is seen from Fig. 4(a) that SLM can lower the PAPR effectively when M is large [10], but the PAPR reduction capability degrades when N_t and/or N_r increases. This is because the minimax criterion reduces the degree of freedom in waveform candidate generation, and hence cannot guarantee the optimal solution at each transmit antenna. Assuming M=256, the PAPR can be reduced by 3.7 dB and 3.2 dB in OFDM-STBC-TD transmission with Tx-FDE when (N_t,N_r)=(2,2) and (4,2), respectively. In addition, it is observed that the PAPR of OFDM transmission using Tx-FDE remains close to that of without Tx-FDE (about 0.1 dB difference when (N_t,N_r)=(1,1)). A possible reason is that Tx-FDE weight multiplication does not cause major effect on the independence among OFDM subcarriers.

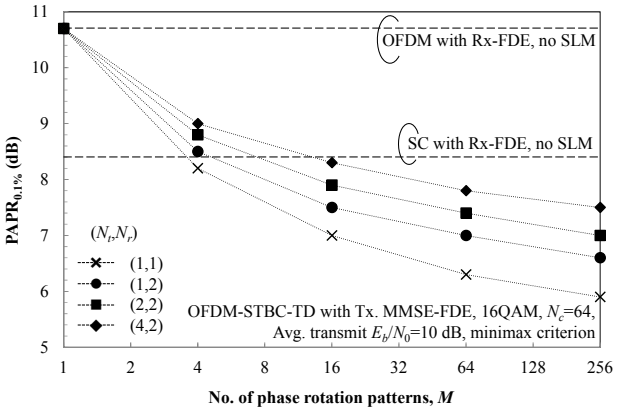

(a) OFDM transmission

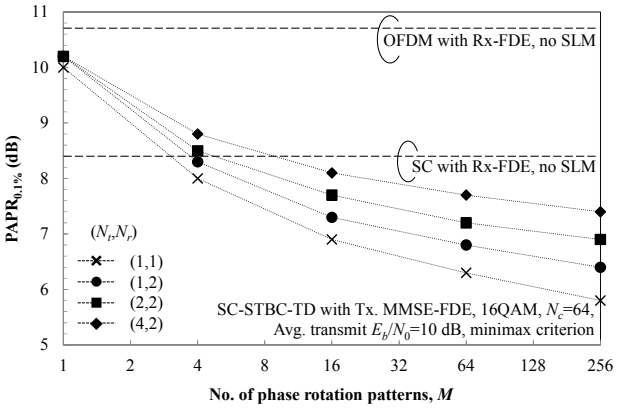

(b) SC transmission

Fig. 4 $PAPR_{0.1\%}$ versus the number of candidates.

Meanwhile, in Fig. 4(b), it is seen that the use of Tx-FDE increases PAPR by 1.6 dB when $(N_t,N_r)=(1,1)$ in SC transmission, although it is still 0.7 dB lower than that of OFDM. A supporting reason of an increasing in PAPR when Tx-FDE is used was already described in [12-13] that Tx-FDE weight multiplication leads to pre-distortion in the frequency spectrum of SC signal, making the transmit spectrum become close to that of OFDM signal. However, the simulation results confirm that SLM can effectively reduce the PAPR of SC-STBC-TD with Tx-FDE. SLM can lower the PAPR by 3.3 dB and 2.8 dB in SC-STBC-TD with Tx-FDE when $(N_t,N_r)=(2,2)$ and (4,2), respectively, and assuming $M=256$. It is also seen that PAPR increases when N_t increases due to the disadvantage of minimax criterion, which is similar to the case of OFDM-STBC-TD.

In addition, there exists an important observation obtained from Fig. 4 that the difference of PAPR between OFDM-STBC-TD using Tx-FDE and SC-STBC-TD using Tx-FDE is very small when N_t and M are large, i.e., only 0.1 dB difference when $(N_t,N_r)=(4,2)$ and $M=256$. This observation means that there is no significant advantage in aspects of PAPR whether OFDM-STBC-TD or SC-STBC-TD are used when Tx-FDE is also considered.

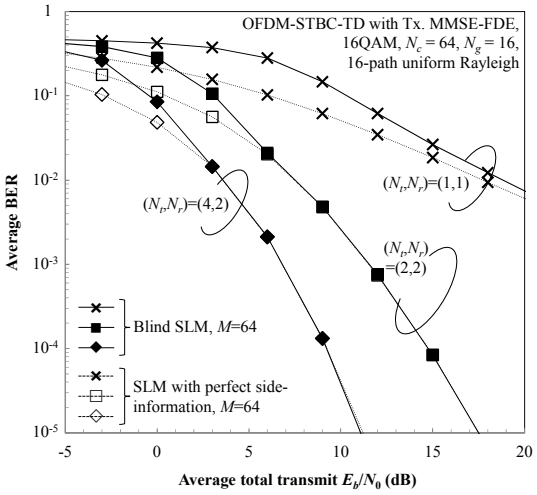

(a) OFDM transmission

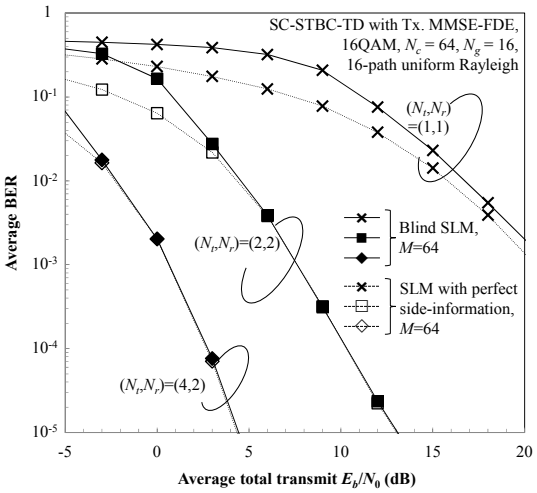

(b) SC transmission

Fig. 5 BER performances.

4.2. BER performance

Fig. 5 shows the uncoded BER performances of STBC-TD with Tx-FDE and blind SLM as a function of total transmit $E_b/N_0=(1/N_{\mathrm{mod}})(E_s/N_0)(1+N_g/N_c)$ with N_{mod} represents modulation level (4 for 16QAM). Performances of OFDM transmission and SC transmission are plotted in Figs. 5(a) and 5(b), respectively. The number of transmit and receive antennas for STBC-TD (N_t,N_r) is assumed to be (1,1), (2,2) and (4,2). BER of STBC-TD with Tx-FDE and SLM with side-information transmission is also provided for comparison, where the side-information detection is assumed to be ideal. The number of phase rotation sequence is set to be $M=64$.

It is seen from Fig. 5 that BER improves when either N_t or N_r increases due to an increasing of spatial diversity gain. The BER of SC-STBC-TD (shown in Fig. 5(b)) is better than that of OFDM-STBC-TD in every (N_t,N_r) case. This is because the combination of SC transmission and MMSE-FDE contributes to frequency diversity gain [14] regardless of the whether the FDE is applied at the transmitter or the receiver. The BER performances of

transmissions using blind SLM degrades compared to those of transmissions using with SLM with ideal side-information detection when the transmit power is low. This is consistent with [8-10] since the noise power makes the received symbols become apart from the original constellation even though the de-mapping is correctly carried out. However, it is seen that there is no difference on BER of blind SLM and SLM with side-information sharing, both OFDM-STBC-TD and SC-STBC-TD, when the transmit power is sufficiently high.

In summary, although the results in Sect. 4.1 indicate that there is no significant advantage in aspect of PAPR between OFDM-STBC-TD and SC-STBC-TD with Tx-FDE and blind SLM, the simulation result shown by Fig. 5 mentions that SC-STBC-TD can be considered as a better option than OFDM-STBC-TD in terms of uncoded BER performance. However, the BER performance of STBC-TD with Tx-FDE, blind SLM and forward error-correction coding (FEC) has not been yet considered. Therefore, the performance evaluation considering FEC is left as our important future work.

5. Conclusion

Blind SLM technique for STBC-TD with Tx-FDE was introduced in this paper. The SLM employs a selected common phase rotation pattern for all N_t transmit antennas, while it selected based on minimax criterion. An arbitrary number of N_t can be used without reducing STBC code rate. Computer simulation results confirmed that the SLM can lower the PAPR of both OFDM and SC signal by 2.8-3.7 dB when M=256 and N_t=2 or 4. It is also shown that no significant BER degradation occurs even though there is no side-information transmission.

Acknowledgement

This paper includes a part of results of “The research and development project for realization of the fifth-generation mobile communications system” (#0155-0019, April 2016) commissioned to Tohoku University by The Ministry of Internal Affairs and Communications (MIC), Japan.

References

[1] DOCOMO 5G White Paper, 5G Radio Access: Requirements, Concept and Technologies, Jul. 2014 (https://www.nttdocomo.co.jp/english/corporate/technology/whitepaper_5g/).

[2] W. L. Chan and J. R. Long, “A 58-65 GHz Neutralized CMOS Power Amplifier with PAE above 10% at 1-V Supply,” *IEEE Journal of Solid-State Circuits*, Vol. 45, No. 3, pp. 554-564, Mar. 2010.

[3] H. G. Myung, J. Lim and D. J. Goodman, “Single Carrier FDMA for Uplink Wireless Transmission,” *IEEE Veh. Technol. Mag.*, Vol. 1, No. 3, pp. 30-38, Sept. 2006.

[4] A. Boonkajay and F. Adachi, “Selected Mapping Technique for Reducing PAPR of Single-Carrier Signals,” *Wireless Commun. Mobile Comput.*, Vol. 16, Issue 16, pp. 2509-2522, Nov. 2016.

[5] R. W. Bauml, R. F. H. Fischer and J. B. Huber, “Reducing the Peak-to-Average Power Ratio of Multicarrier Modulation by Selected Mapping,” *IEEE Electron. Lett.*, Vol. 32, No. 22, pp. 2056-2057, Oct. 1996.

[6] A. Boonkajay and F. Adachi, “A Blind Selected Mapping Technique for Low-PAPR Single-Carrier Signal Transmission,” *in Proc. Int. Conf. Info. Commun. and Signal Process. (ICICS2015)*, Singapore, Dec. 2015.

[7] A. Boonkajay and F. Adachi, “A Blind Polyphase Time-Domain Selected Mapping for Filtered Single-Carrier Signal Transmission,” *in Proc. IEEE Veh. Technol. Conf. (VTC2016-Fall)*, Montréal, Canada, Sept. 2016.

[8] A. Boonkajay and F. Adachi, “2-Step Signal Detection for Blind Time-Domain Selected Mapping,” *IEICE Tech. Rep.*, Vol. 116, No. 257, RCS2016-182, pp. 161-166, Oct. 2016.

[9] S. M. Alamouti, “A simple transmit diversity technique for wireless communications,” *IEEE J. Select. Areas. Commun.*, Vol. 16, No. 8, pp. 1451-1458, Oct. 1998.

[10] A. Boonkajay and F. Adachi, “Blind Selected mapping Techniques for Space-Time Block Coded Filtered Single-Carrier Signals,” *in Proc. IEEE VTS Asia Pacific Wireless Commun. Symp. (APWCS2016)*, Tokyo, Japan, Aug. 2016.

[11] H. Tomeba, K. Takeda and F. Adachi, “Frequency-domain Space-Time Block Coded-Joint Transmit/Receive Diversity for Direct-Sequence Spread Spectrum Signal Transmission ,” *IEICE Trans. Commun.*, Vol. E90-B, No. 3, pp. 597-606, Mar. 2007.

[12] A. Boonkajay, T. Obara, T. Yamamoto and F. Adachi, “Selective Mapping for Broadband Single-Carrier Transmission Using Joint Tx/Rx MMSE-FDE,” *in Proc. IEEE 24th Int. Symp. on Personal Indoor and Mobile Radio Commun. (PIMRC2013)*, London, United Kingdom, Sept. 2013.

[13] S. Kumagai, T. Obara, T. Yamamoto and F. Adachi, “Joint Tx/Rx MMSE Filtering for Single-Carrier MIMO Transmission,” *IEICE Trans. Commun.*, Vol. E97-B, No. 9, pp. 1967-1976, Sept. 2014.

[14] D. Falconer, S. L. Ariyavisitakul, A. Benyamin-Seeyar and B. Edison, “Frequency Domain Equalization for Single-Carrier Broadband Wireless Systems,” *IEEE Commun. Mag.*, Vol. 40, No. 4, pp. 58-66, Apr. 2002.